M. G. Dunn

P. J. Seymour

Calspan Advanced Technology Center,
Buffalo, NY 14225

S. H. Woodward

W. K. George

State University of New York at Buffalo,
Buffalo, NY 14225

R. E. Chupp
Teledyne CAE
Toledo, OH 43612

Phase-Resolved Heat-Flux Measurements on the Blade of a Full-Scale Rotating Turbine

This paper presents detailed phase-resolved heat-flux data obtained on the blade of a Teledyne 702 HP full-stage rotating turbine. A shock tube is used as a short-duration source of heated air and platinum thin-film gages are used to obtain the heat-flux measurements. Results are presented along the midspan at several locations on the blade suction and pressure surfaces from the stagnation point to near the trailing edge. For these measurements, the turbine was operating at the design flow function and at 100 percent corrected speed. Results are presented for the design vane/blade spacing ($0.19\,C_s$) and at a wide spacing ($0.50\,C_s$). Data are also presented illustrating the phase-resolved blade heat-flux distribution with upstream cold gas injection from discrete holes on the vane surface. The results illustrate that several successive passages can be superimposed upon each other and that a heat-flux pattern can be determined within the passage. A Fourier analysis of the heat-flux record reveals contributions from the fundamental and first harmonic of the passage cutting frequency. Time-resolved surface pressure data obtained on the blade pressure surface are compared with heat-flux data.

1 Introduction

Turbomachinery flow fields are inherently unsteady because of the disturbances generated when rotating blades transit nozzle vane wakes and exit passages. Years of experience has illustrated that these flows can be considered to be quasi-steady and satisfactory flow field predictions can be performed. However, the state of the art has progressed to the point where relevant unsteady calculations can now be performed and supporting measurements of the unsteady flow field can be made. Significant current research is directed at determining the influence of flow-field unsteadiness on the blade heat-flux and surface-pressure distributions, on the inner blade-row gas-dynamic parameters, on the state of the blade and vane surface boundary layers, and on the stage efficiency. The results reported in this paper will emphasize phase-resolved[1] heat-flux data on the rotating blade and will demonstrate the influence of vane/blade spacing and cold gas injection on these phase-resolved data. Limited time-resolved surface pressure data obtained on the rotating blade will also be presented.

Papers relevant to unsteady flow fields in turbomachinery have been present in the literature for at least the past 35 years. Early work by Kemp and Sears (1953, 1955) provided the ground work for much of the research that was to follow. Subsequently, Giesing (1968), Parker (1969), and Kerrebrock and Mikolajczak (1970) made valuable contributions to the understanding of these problems. More recently, Dring et al. (1980, 1981, 1982) have used a large-scale rotating axial turbine stage to obtain valuable experimental data on the nature of the unsteady flow field. Also, Hodson (1984, 1985a, 1985b) has used several different facilities to study wake-generated unsteadiness in vane exit passages and to perform measurements of boundary-layer transition and flow separation. Detailed measurements of the unsteadiness in the rotor incoming flow are presented in Hodson (1985b) that illustrate the change in incidence angle and the change in turbulence associated with the vane wakes.

Another extensive research program concerned with unsteady flow fields was reported by Gorton and Lakshminarayana (1976). They reported the results of several programs designed to measure the boundary-layer and turbulence characteristics inside turbomachinery rotor passages using a large-scale, slowly rotating rig as the test device. Binder et al. (1985, 1987) reported the results of laser velocimeter measurements in the unsteady rotor flow field. These authors demonstrate very high turbulence levels associated with the vane wakes. Sharma et al. (1985) presented the results of an extensive study conducted to obtain low-speed rig data on the unsteady flow environment associated with axial flow turbines. Doorly and Oldfield (1985) used a piston-driven tunnel and a system of rotating bars to simulate

[1] The term "phase" is used here to denote the pitchwise angular displacement of a given rotor blade with respect to the stator vanes. It varies across each stator passage, in a sawtooth fashion, between the limits zero and 360 deg /B, where B is the number of stators. The term "phase resolved" denotes time-resolved data that are presented as a function of phase, rather than as a function of time. The term "phase averaged" denotes an ensemble average in which phase-resolved data at a given phase, over a succession of stator passages, are taken to be different realizations of the same event. This averaging is referred to by Adamczyk (1985) as passage-to-passage averaging.

Contributed by the International Gas Turbine Institute and presented at the 33rd International Gas Turbine and Aeroengine Congress and Exhibition, Amsterdam, The Netherlands, June 5-9, 1988. Manuscript received by the International Gas Turbine Institute June 1987. Paper No. 88-GT-173.

the effects of shock waves and wakes shed from a nozzle on the blade. The Schlieren photographs presented by Doorly and Oldfield (1985) are helpful in interpreting the results presented herein because they illustrate the rather extensive nature of the vane wake, and the manner in which these wakes interact with the blade.

The purpose of this paper is to present a detailed set of phase-resolved heat-flux data obtained on the blade of the Teledyne CAE full-stage rotating turbine. For several blade locations, the predicted heat-flux values are compared here to the measured phase-dependent heat flux. Two previous papers by Dunn and Chupp (1987, 1988) have described in detail the steady-state gas-dynamic parameters and Stanton number distributions for this turbine. In Dunn and Chupp (1988), the distribution of nozzle inlet and rotor exit total pressure and total temperature, the stage static pressures, the turbine operating conditions, the steady-state vane and blade Stanton number distributions, and comparisons of these distributions with various prediction techniques were all presented. In Dunn and Chupp (1987), the influence of vane/blade spacing on the steady-state vane and blade Stanton number distributions at two different spacings (0.19 C_s and 0.50 C_s), with and without discrete hole injection, was presented. While the measurements noted above were being performed, the time-resolved (or phase-resolved) data reported in this paper were also being obtained. Two earlier papers (Dunn et al., 1986; George et al., 1987) provide a description of the analysis techniques that were previously developed at the Calspan–UB Research Center to obtain instantaneous heat-flux values from the thin-film gages at a sampling frequency consistent with the requirements of this experiment. Several changes have been made to the electronics of the data recording system since the experimental data reported by Dunn et al. (1986) were taken. These changes were incorporated into the data collection system used for this work and they will be described later in this paper. Previous papers by Dunn et al. (1986), Dunn and Hause (1982), Dunn et al. (1984a), and Dunn (1986) have described time-resolved rotor shroud pressure and time-resolved blade heat-flux measurements for a different turbine, the Garrett TFE 731-2 HP.

2 Experimental Apparatus

The experimental apparatus used in this work has previously been described in depth and will not be repeated here. Only those portions of the apparatus important to the clarity of this paper will be included.

The high-pressure turbine stage was taken from a Teledyne J402-CA-702 turbojet engine. The turbine stage of this engine is a highly loaded, moderately high reaction, state-of-the-art design with an aspect ratio near unity. The corrected speed is 19,510 rpm, the corrected weight flow is 3.92 lb/s, and the overall total-to-total pressure ratio is 3.62. There are 23 nozzle guide vanes, which are convectively cooled and have pressure-side and suction-side discrete hole injection. The injection on each side is from a single spanwise row of circular cooling holes. The turbine has 35 uncooled blades, which are highly tapered, highly cambered, and have elliptical leading edges. The model constructed to house the turbine stage was designed so that the vane/blade spacing could be either 0.19 C_s (close spacing) or 0.50 C_s (wide spacing). The spacing was increased by moving the nozzle forward and inserting a spacer to provide the proper air seal between the vane exit and the rotor entrance.

The thin-film gage instrumentation used to perform the measurements described here consisted of contoured leading-edge inserts and flush-mounted button-type gages. The instrumentation was concentrated on the blade meanline but a few measurements were obtained at other selected locations as described in Dunn and Chupp (1988). Heat-flux measurements were obtained for 21 locations on the vane and for 45 locations on the blade.

Figure 1 is a photograph of one of two blade-leading-edge inserts. Each insert had 12 gages, with the distribution of gages selected so that one insert provided a close spacing on one surface (on the order of 1 mm or 0.040 in.) and a wider spacing on the other surface. The second insert has a close gage spacing on the side for which the first insert had a wide spacing. Each of these inserts was contoured to the blade leading-edge profile prior to painting the thin-film gages. The particular insert shown in Fig. 1 contains one gage at the geometric stagnation point, eight gages on the suction surface, and three on the pressure surface.

For the rotor speeds used here (27,000 rpm), a blade traverses a vane passage in 97 μs, which corresponds to a wake-cutting frequency of approximately 10 kHz. However, in order to sample these data properly as described in Dunn et al. (1986), the overall system frequency response must be substantially greater than 10 kHz. The frequency response of the system used here was limited by the bandwidth of the gage follower amplifiers and subsequent low pass filters, which for this experiment were set with the -3 dB point at 100 kHz.

The output from the gage amplifiers was directly recorded on two 10-bit transient recorders, a Data Laboratories 2000 series and a Physical Data 515A. Both of these were eight-channel units with a storage capability of 4K words/channel and could be sampled at a frequency in the 200 kHz to 2 MHz range. The sampling on these devices was controlled by means of a shaft encoder installed on the rotor assembly providing 720 pulses per revolution and one pulse per revolution. At the time of model assembly, the leading edge of one of the inserts was carefully aligned with the trailing edge of a known vane, as will be described in Section 5.1. The shaft encoder was then adjusted so that the one pulse per revolution always occurred at this alignment point. The vane passages are then 15.65 deg or 31.3 pulses apart. The output signal from the shaft encoder was used as an input to the recording equipment in order to sample the blade data at the same angular location within the passage from one revolution to the next, thus phase resolving the data. This technique resulted in an average sampling frequency on the order of 315 kHz, a value well above twice the highest frequency as required by the Nyquist criterion. The recorder used to store these data had capacity for 4000 words/channel. Therefore, it was possible to record two and

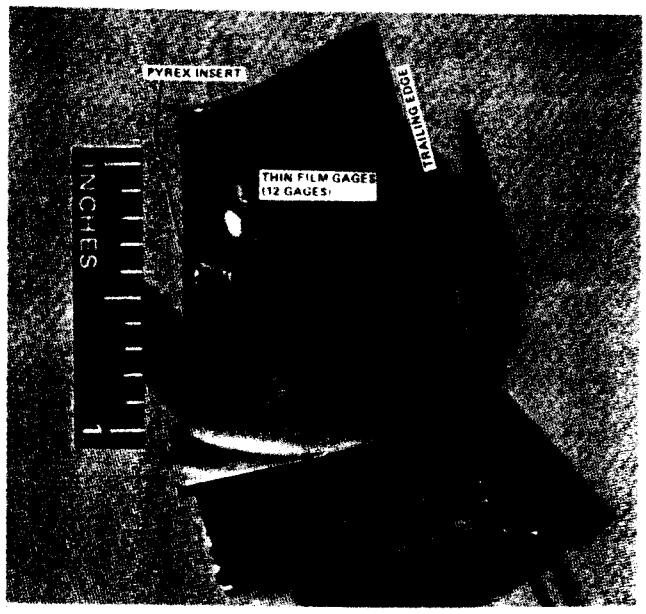

Fig. 1 Photograph of blade suction surface leading edge insert

one half to three rotor revolutions during the test-time duration. One channel of the recorder was used to record a 10 kHz timing pulse in the form of a ramp signal in order to derive the arrival time of each encoder pulse. The absolute time and angular location of each sample is then known.

Dunn et al. (1986) noted that some of the features of the data could not be readily explained by the analysis and that electronic noise combined with frequency splitting due to sampling the slightly accelerating turbine data at constant time intervals made it difficult to recognize the character of the passage heat flux easily. Therefore, prior to obtaining the results reported here, the electronic system and the amplifiers used in the thin-film gage temperature recording circuits were redesigned and rebuilt. These amplifiers were constructed to provide capability of wide band (200 kHz), low noise (less than 3 bits out of 1024 bits), single gain data recording and were powered by d-c voltage (batteries). Great care was taken in providing electrical shielding and adequate grounding for all of the equipment. Where possible, batteries were used as the power supply for the electronic equipment. The noise level on each individual heat-flux gage channel was measured through the entire recording system (including the slip ring) with the turbine rotating. For all channels, the prerun system noise measured at the recording device just prior to recording the data (with the turbine at full speed) was less than 5 bits out of 1024 bits. Throughout the measurement program, an attempt was made to use as large a portion of the 1024 bits as possible for data recording. Figure 2 is a schematic of the data recording system used in this work. For the data presented here, the number of bits utilized on any given channel ranged from 600 to 1000. In several cases, the data range for a particular channel was from 10 to 1000 bits.

3 Data Processing

The technique for recording the unsteady heat-flux values from the phase-sampled gage temperature data was shown schematically in Fig. 2. The digital surface temperature data were converted to unsteady heat flux by utilizing the simple implicit code described by Dunn et al. (1986). No attempt was made to correct the heat-flux data presented here for variable substrate thermal properties. For the purposes of this paper, this correction is estimated to be generally less than 10 percent. The algorithm and a detailed analysis of the simple implicit procedure are presented by George et al. (1987). Briefly, it was concluded that the effective frequency response of the simple implicit code (as determined by the frequency at which the calculated heat flux is 3 dB below the actual value) was one fourth of the rate at which the temperature data were sampled. Thus in the work reported here, the effective bandwidth of the calculated heat flux was approximately 80 kHz, well above the frequency at which quantization and electronic noise would mask the vane-crossing harmonics.

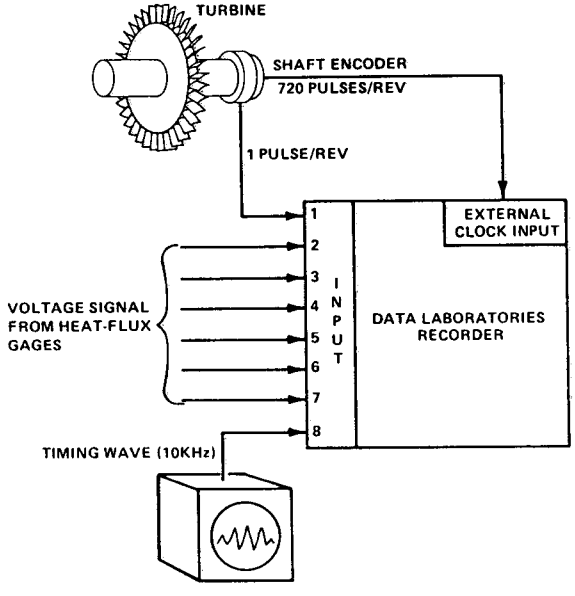

Fig. 2 Schematic of data recording system

In order further to reduce the effect of the quantization errors and electronic noise on the calculated heat flux, the sampled temperature data were digitally filtered with a simple five-point top-hat filter before utilization in the simple implicit code. This further reduced the effective bandwidth to approximately 65 kHz. This bandwidth was sufficient to capture all of the harmonics present in the original signal as clearly evident from the spectra of the directly recorded data.

4 Experimental Conditions

A table giving the experimental conditions at which the measurements reported here were performed is given in both Dunn and Chupp (1987, 1988) and will not be repeated here. A detailed description of the vane/blade spacing and coolant gas injection parameters was also given. The turbine was operating at nearly the design values of corrected speed, flow function, and total-to-total pressure ratio. The temperature of the injected coolant gas was always 530 R and the total temperature of the free-stream gas was always about 1010 R. The metal surface temperature of the stage components was always nearly equal to 530 R. For this particular turbine, the incoming turbulence intensity was not measured. However, for a comparable experiment, Dunn et al. (1984b) measured the turbulence intensity upstream of the vane row to be about 5 percent. The actual engine values are unknown but estimates in the range of 10 to 20 percent are common.

5 Discussion of Results

A typical thin-film gage temperature history for one revolution at a blade suction-surface location of 14.9 percent wetted distance is given in Fig. 3. For a constant heat-flux input to the gage, the temperature history should have a parabolic shape as illustrated by this figure. The nozzle has 23 vanes, so that for one revolution of the rotor, one observes 23 distinct events, as illustrated in Fig. 3. It can be seen from this thin-film gage temperature history that not all passages produce the identical exit flow. This can be caused by many different factors including turbulence and unsteady flow, as well as the fact that the components used here are actual engine hardware and some manufacturing variation must be expected. Figure 4(*a*) is the heat-flux history calculated from the temperature history described above using the techniques reported by George et al. (1987). Once again, 23 distinct passages are obvious from the heat-flux history for the single rotor revolution. The experiment is structured so that the rotor completes several revolutions during the useful test time, as has been explained in previous publications. Note that the excursion of the heat flux about an average value is significant, but the heat flux is always positive. Plots for other rotor revolutions within the test time and for different blade locations are similar to those shown here.

Figure 4(*b*) is an example of the revolution to revolution reproducibility of the heat-flux history. The data shown on this figure were obtained at 10 percent wetted distance on the blade suction surface for the case of close spacing with vane injection (see Fig. 12 for a more detailed description of results obtained at his particular location). Figure 4(*b*) is presented for one-half revolution so as to illustrate the nature of the flow. Even though the passage-to-passage and revolution-to-revolution details are not reproduced exactly, the overall characteristics of the passage signature are reproduced.

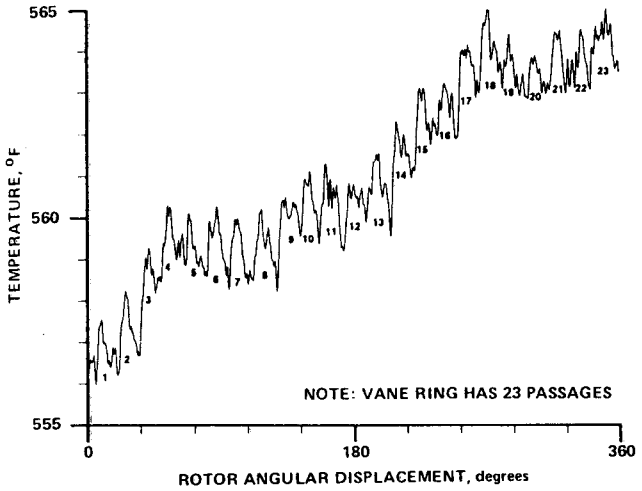

Fig. 3 Thin-film gage temperature history on blade for one revolution of the rotor

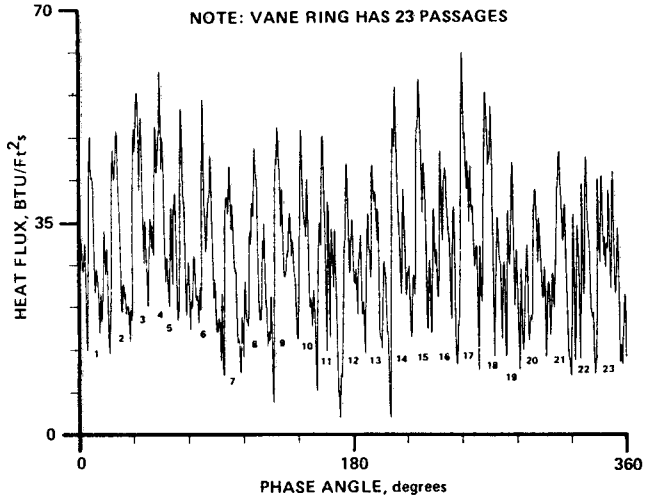

Fig. 4(a) Heat-flux history for one revolution

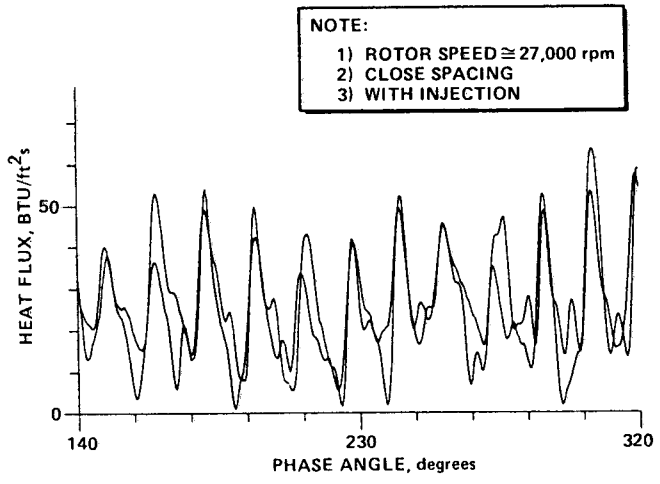

Fig. 4(b) Heat-flux history for two revolutions obtained at 10 percent wetted distance on blade suction surface (see Fig. 12)

Phase-resolved heat-flux data obtained from the instrumented blades will be presented for the cases of: (*a*) close spacing, no injection, (*b*) close spacing, with injection, and (*c*) wide spacing, with injection. An illustration of the time-resolved surface pressure data obtained on the blade pressure surface will also be presented.

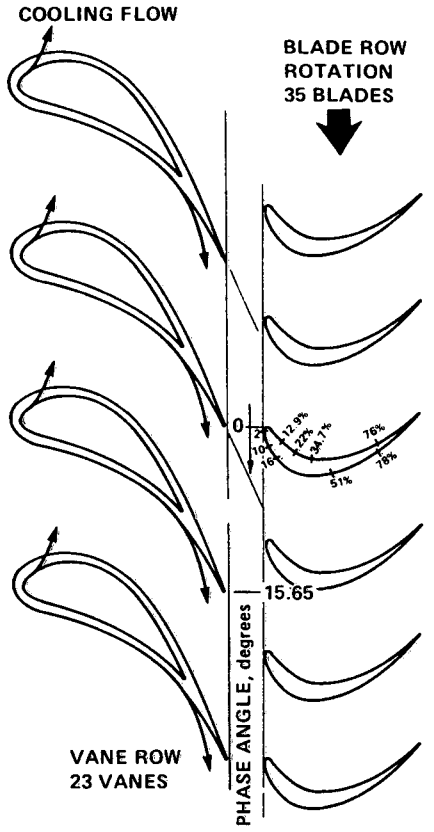

Fig. 5 Sketch of stage and phase angle reference

5.1 Phase-Resolved Heat-Flux Data for Close Spacing in the Absence of Injection. Heat-flux measurements were obtained at several spanwise locations on the blade but the results described herein will be confined to the blade midspan region. As stated previously, the shaft encoder was aligned during model assembly to provide a single pulse each time the blade containing the insert shown to Fig. 1 passed a particular location relative to the vane trailing edge. Thus, by knowing the geometry of the stage, the relative location of the blade with respect to the vane wake can be determined in order to resolve the wake and passage flow. A sketch of the physical arrangement of the vane, blade, and the orientation of the blade at 0 deg and 15.65 deg phase (360 deg/23 vanes) is given in Fig. 5. This alignment procedure is consistent with that used by Dring et al. (1982), thus permitting direct comparison of the results. An extension of the vane mean camber line illustrates that the approximate centerline of the wake would intersect the blade at a phase angle of about 7.6 deg. Exactly where the vane wake is located with respect to the blade phase angle is difficult to predict for this unsteady environment.

It was noted earlier that there are 45 heat-flux gages on the instrumented blades but that space permits discussion of only a few. The specific gages that were utilized to obtain the results presented here were located at the geometric stagnation point, 2.1, 10, 16, 51, and 78 percent wetted distance on the suction surface, and 12.7, 22, 34.7, and 76 percent wetted distance on the pressure surface. These gage locations are denoted on the sketch in Fig. 5.

The heat transfer data presented in this paper will be given in the form of heat-flux (BTU/ft²s) history as a function of phase angle instead of in the form of the nondimensional Stanton or Nusselt number. However, the authors recognize that some may prefer the nondimensional format, so Table 1 is given to provide all of the parameters necessary for the conversion from heat flux to Stanton or Nusselt number.

Table 1 Teledyne 702-HP flow parameters

Vane inlet total temperature	561°K	1010°R
Vane inlet total pressure	6.67 x 10^2k Pa	96.8 psia
Vane inlet static pressure	6.60 x 10^2k Pa	95.7 psia
Approximate weight flow	8.61 kg/s	19 lb/s
Wall temperature	294°k	530°R
Rotor inlet relative total pressure	3.29 x 10^2k Pa	47.8 psia
Rotor inlet relative total temperature	476°K	847°R
Rotor inlet relative velocity	158.6 m/s	520 ft/s

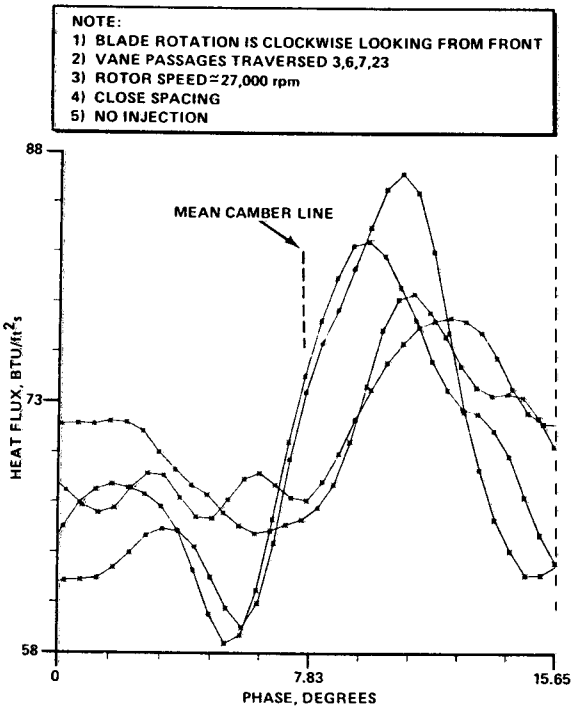

Fig. 6(a) Phase-resolved heat-flux data at geometric stagnation point on blade

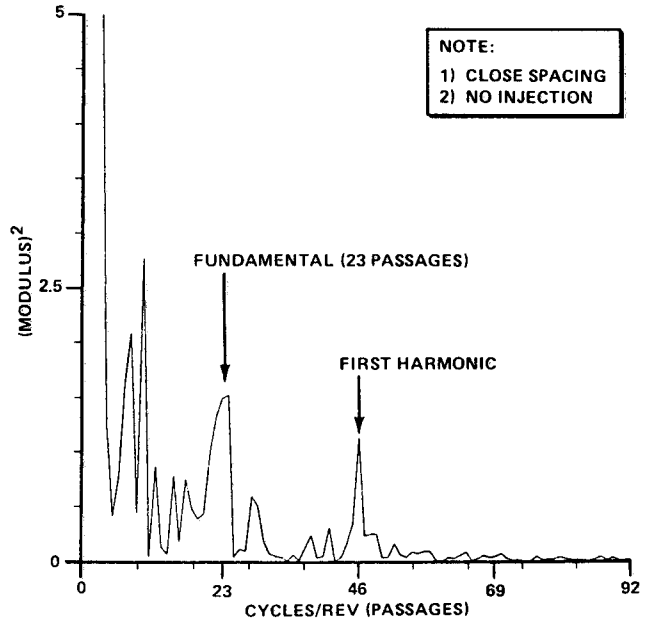

Fig. 6(b) Modulus of Fourier transform of heat-flux data at geometric stagnation point on blade

Figure 6(a) presents the passage phase-resolved heat-flux history for the blade geometric stagnation point. Data from four different passages have been overlaid on this plot to provide an illustration of the passage heat-flux history. As

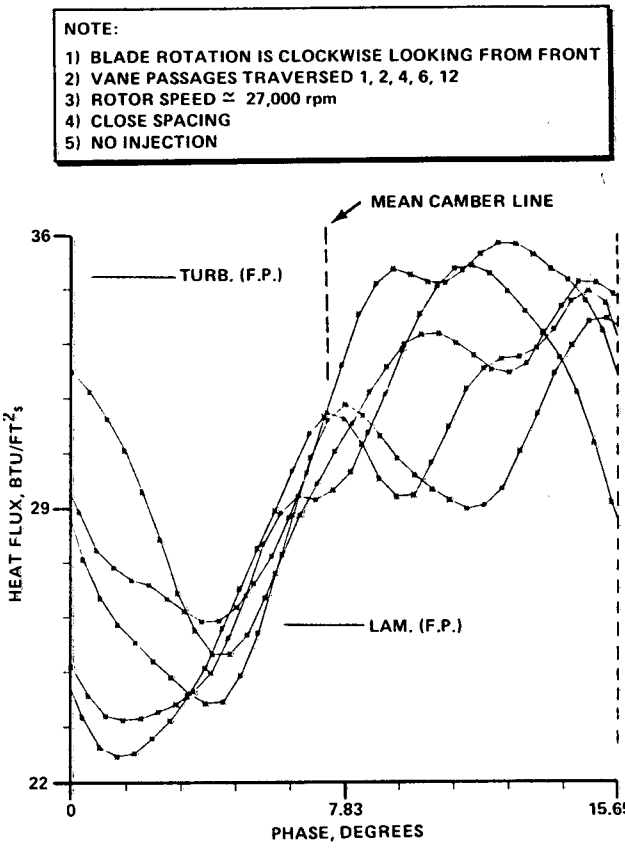

Fig. 7(a) Phase-resolved heat-flux data at 2.07 percent wetted distance on blade suction surface

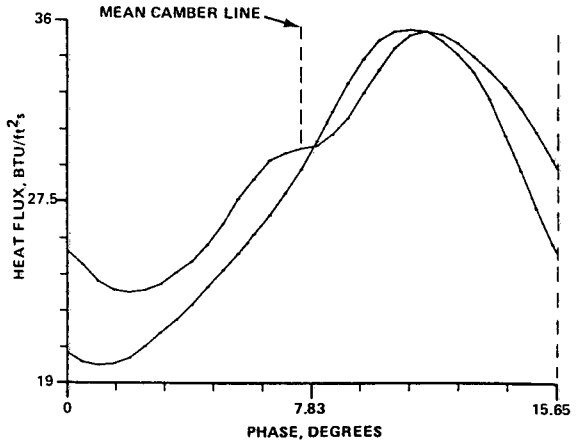

Fig. 7(b) Phase-resolved heat-flux data at 2.07 percent wetted distance on blade suction surface for passage #1 on successive revolutions

previously noted, the passage separation is approximately 15.65 deg, which results in 31.3 data points per passage for an encoder with 720 pulses/rev. The blade is rotating clockwise when viewed from the front at a speed of nearly 27,000 rpm. On all of the plots presented in Fig. 6(a), 7, 8(a), 9(a), 10, 11(a), and 12(a) the phase position 0 deg corresponds to the initial blade/vane alignment illustrated in Fig. 5 and the phase position 15.65 deg corresponds to the arrival of the blade at the next vane. The location of the intersection of the vane mean camber line with the plane of the blade leading edge is noted on Fig. 6(a), 7, 8(a), 12(a), and 13(a). Previous work by Dring et al. (1985) using photographs with smoke in the free-stream flow and the detailed rotating bar measurements of Doorly and Oldfield (1985) have illustrated the nature of the vane trailing edge wake. In addition, there are probably

several interacting vortex flows coming through the passage flow. The extent of these disturbances is not well known for a three-dimensional, compressible turbine flow of the type used here and some definition of their influence on the blade heat-flux distribution is a portion of the intent of this work.

The ordinate on Fig. 6(*a*) has been expanded to illustrate the variation in heat flux. Note that the scale begins at 58 and goes to 88 Btu/ft^{2}s. The heat-flux level is lowest in the vicinity of 0 deg phase angle, which presumably corresponds to flow outside the vane wake and remains relatively low for the initial 6 deg of the passage and then begins to increase rapidly, reaching a peak in the vicinity of 10.3 deg, and then falls off again. An extension of the vane mean camber line as shown on Fig. 5 would suggest that the blade would intercept this wake flow at about 7.6 deg. The rapid increase in heat flux near 6 deg is consistent with this interaction. The stagnation-point flow is unsteady as the blade moves from passage to passage. However, the general characteristics of the passage distribution are repeatable showing the peak heat flux occurring in the vicinity of 10 deg and then falling off rapidly. There appears to be a broader region of increased heat flux associated with the flow in the region of the wake location suggesting that the wake region is not a small, well-defined one at this location, consistent with the visual observations of Doorly and Oldfield (1985). This same general pattern will be shown for the initial four locations on the suction surface, but it will change for the pressure surface. Figure 6(*b*) is the modulus squared of the FFT[2] of a single record of the stagnation point heat-flux data

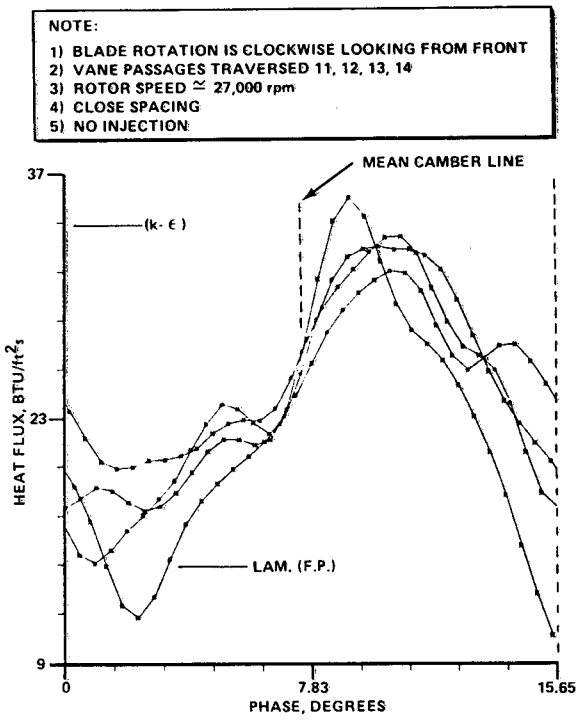

Fig. 8(*a*) Phase-resolved heat-flux data at 10 percent wetted distance on blade suction surface

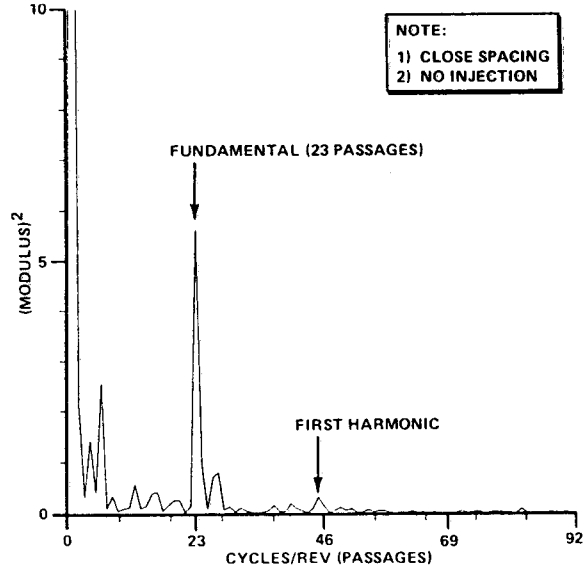

Fig. 8(*b*) Modulus of Fourier transform of heat-flux data at 10 percent wetted distance on blade suction surface

[2]The phrase "modulus of the FFT" is used to refer to the modulus of the Fourier series coefficients obtained by an FFT algorithm. The square of the modulus corresponds to the Fourier line spectrum of the data record.

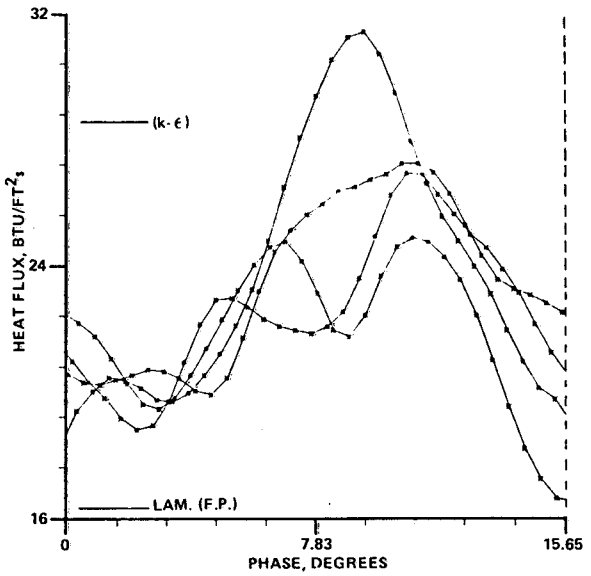

Fig. 9(*a*) Phase-resolved heat-flux data at 16.1 percent wetted distance on blade suction surface

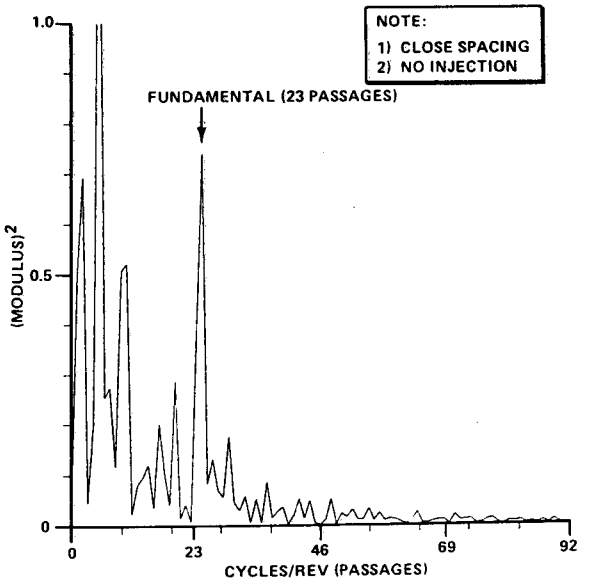

Fig. 9(*b*) Modulus of Fourier Transform of heat-flux data at 16.1 percent wetted distance on blade suction surface

illustrating a relatively broad peak in the distribution at 23 cycles/rev and the first harmonic at 46 cycles/rev. As noted earlier, there are 23 passages in the nozzle so one would expect to see a significant peak in the modulus at 23 cycles/rev. As discussed in Dunn et al. (1986), the lower frequency peaks are associated with the short-duration nature of the experiment and the unsteady nature of the flow.

Figure 7(*a*) presents a phase-resolved distribution of heat flux for a location of 2.07 percent wetted distance on the blade suction surface and includes the steady-state predicted heat-flux values taken from Dunn and Chupp (1988) for the flat-plate case. The ordinate on Fig. 7(*a*) has again been expanded in order to illustrate the heat-flux variation. The general characteristic of the heat-flux history is similar to that seen for the stagnation-point gage. Four of the five passages shown on Fig. 7(*a*) have a suppressed heat-flux value in that portion of the flow corresponding to the initial 4.6 deg of phase or to the flow that is outside the anticipated vane wake location. At about 5 deg, the heat-flux value increases rapidly reaching a peak in the vicinity of 10 deg as was observed for the stagnation point gage. The fifth passage shown starts out with a heat-flux value at 0 deg that is about 5.5 Btu/ft^{2}s greater than the average of the other four. However, once the blade moves about 5 deg into this passage, the remainder of the profile is very similar. The predicted turbulent flat plate value of heat flux is in reasonable agreement with the peak passage values and the predicted laminar value is in reasonable agreement with the minimum passage values.

It was noted in Section 2 that at the sampling frequency used in this work and because of the necessity to record the early portion of the gage temperature-time history, storage space was available to record two and one half to three rotor revolutions during the useful test time. Figure 7(*b*) shows the phase-resolved heat-flux history for passage #1 obtained for two successive rotor revolutions. The heat-flux levels for the two revolutions are in very good agreement but there is a displacement of about one degree in phase. Review of the phase-resolved data presented in later figures will indicate that passage-to-passage phase displacements on the order of one degree are not unusual.

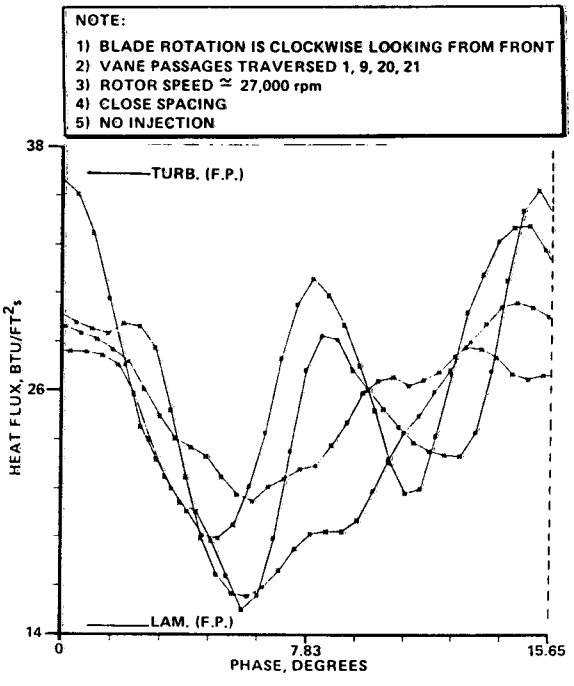

Fig. 10 Phase-resolved heat-flux data at 12.7 percent wetted distance on blade pressure surface

Moving farther along on the suction surface of the blade to 10 percent wetted distance, a heat-flux history very similar to the stagnation-point history was measured and is shown in Fig. 8(*a*) along with the predicted steady-state heat-flux values. For this comparison, the k–ϵ and the laminar flat plate values were used because the turbulent flat plate prediction is known to overpredict the blade suction surface heat flux significantly. The general unsteadiness of the flow at this location is somewhat less than that observed at the 2.07 percent location and the profiles nicely overlay. Again, the trend of the results is for the heat flux to be lowest in the region hypothesized to be outside of the wake. The peak heat-flux values occur at a phase angle in the vicinity of 10 deg as noted for the previous locations. Figure 8(*b*) is the modulus squared

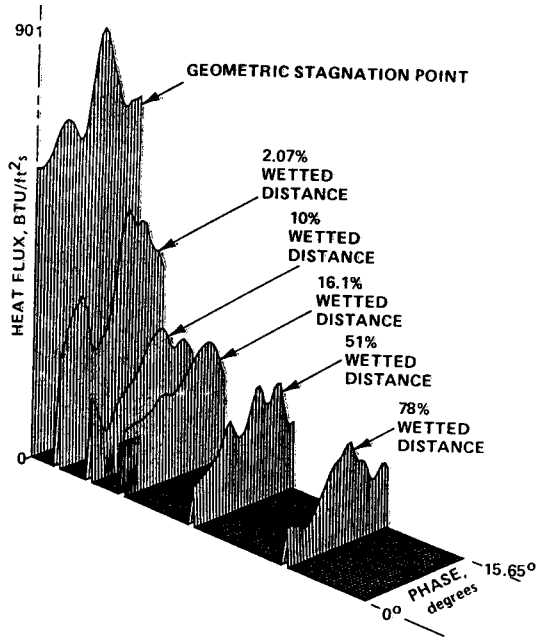

Fig. 11(*a*) Phase-resolved contour plot of heat-flux distribution on blade suction surface

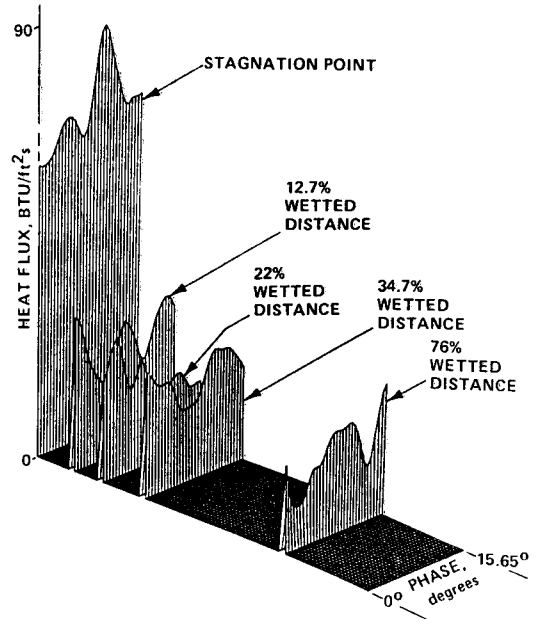

Fig. 11(*b*) Phase-resolved contour plot of heat-flux distribution on blade pressure surface

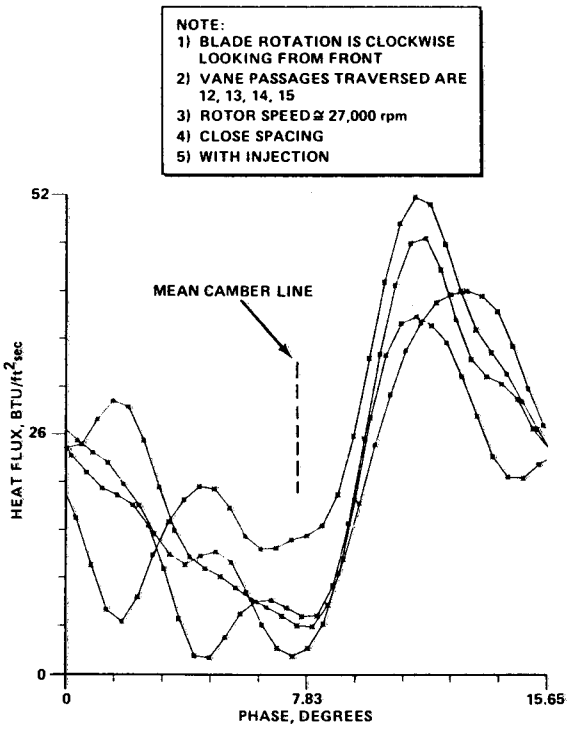

Fig. 12(a) Phase-resolved heat-flux data at 10 percent wetted distance on blade suction surface

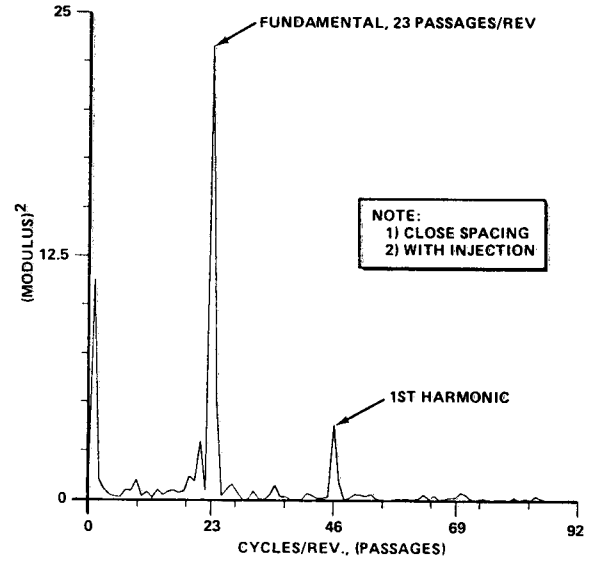

Fig. 12(b) Modulus of Fourier transform of heat-flux data at 10 percent wetted distance on blade suction surface

of the heat-flux data at the 100 percent location and this plot illustrates the strong signal at 23 cycles/rev corresponding to the 23 vanes in the nozzle. The first harmonic is visible, but by this point in the flow its contribution is reduced.

The final location on the suction surface for which detailed results will be presented is at 16.1 percent wetted distance and the phase-resolved heat-flux history is shown in Fig. 9(*a*). The heat flux starts out low as it did at previous locations, but the increase near 5 deg is more gradual than observed closer to the geometric stagnation point. However, the peak heat-flux value continues to occur in the vicinity of 9 deg. Figure 9(*a*) also includes the predicted heat-flux values obtained from the k–ϵ prediction and the laminar flat-plate prediction reported in

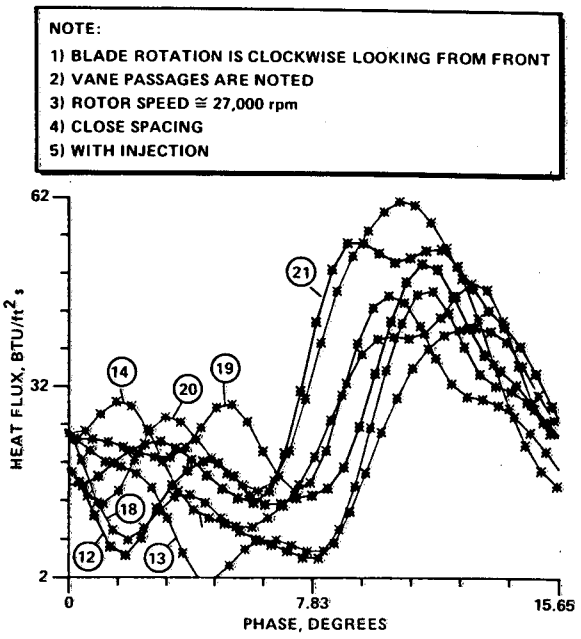

Fig. 12(c) Phase-resolved heat-flux data at 10 percent wetted distance on blade suction surface

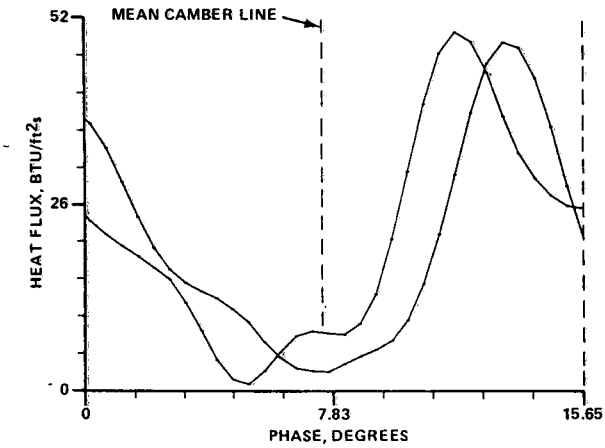

Fig. 12(d) Phase-resolved heat-flux data at 10 percent wetted distance on blade suction surface for passage #13 on successive revolutions

Taulbee et al. (1989). At this particular blade location, the predicted values bound the measured unsteady results. Figure 9(*b*) is the modulus squared of the phase-resolved data illustrating the fundamental at 23 cycles/rev, but the first harmonic is no longer clearly shown. Its absence is consistent with a wake that is becoming less spatially confined as it moves through the passage.

The results presented in Fig. 6–9 suggest that the gages located between 0 and 16 percent on the suction surface all intercepted the vane wake at about the same relative location and reached the peak heat-flux value at about the same location. This trend is consistent with the observations of Dring et al. (1982, 1985) and Doorly and Oldfield (1985). The thin-film rotor data shown by Dring et al. (1982) illustrate a depressed heat-flux value associated with the passage flow and a much broader and considerably greater heat-flux value associated with the vane wake region. A similar picture was described by Doorly and Oldfield (1985), which also included the complication of a shock wave in the flow. In that regard, it should be noted that the vane exit Mach number for the Teledyne 702 turbine used here was slightly greater than 1.0 but the manner

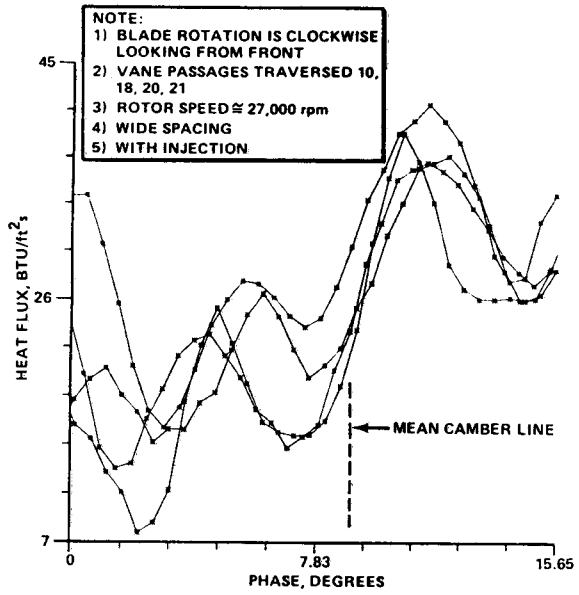

Fig. 13(a) Phase-resolved heat-flux data at 14.9 percent wetted distance on blade suction surface

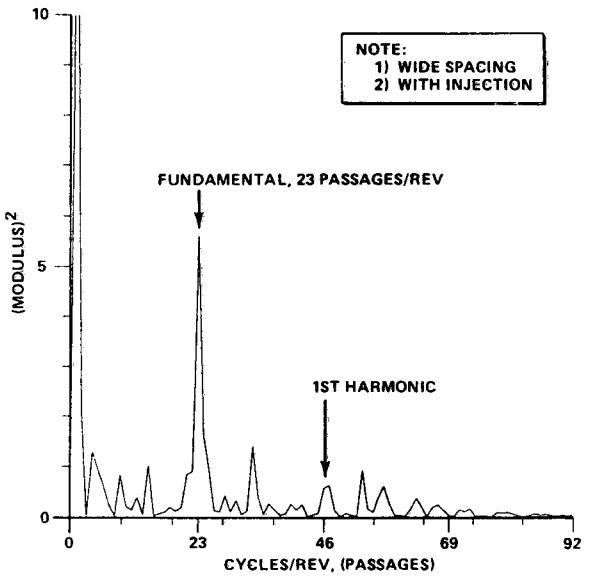

Fig. 13(b) Modulus of Fourier transform of heat-flux data at 14.9 percent wetted distance on blade suction surface

in which potential shock waves interact with the flow field has not been obtained from the data.

The predicted heat-flux values previously reported for this turbine were also noted on Figs. 7–9. Comparison of these predictions with the time-resolved data suggests that the blade boundary layer state was probably fluctuating between laminar and turbulent as the blade interacts with the NGV flow field. This influence of vane rows on the blade boundary layer has previously been described by Evans (1978), Dring et al. (1982), and Doorly and Oldfield (1985).

Figure 10 presents phase-resolved heat-flux data for the blade pressure surface at 12.7 percent wetted distance. All of the gages used to obtain the data reported in Figs. 6(*a*) to 10 were located on the same blade. The pressure surface heat-flux history for the passage is significantly different from the suction surface histories. The heat-flux value over the initial 2 deg is relatively high, but falls rapidly to a minimum in the vicinity of 5 deg and then peaks again near 8 deg. This peak near 8 deg

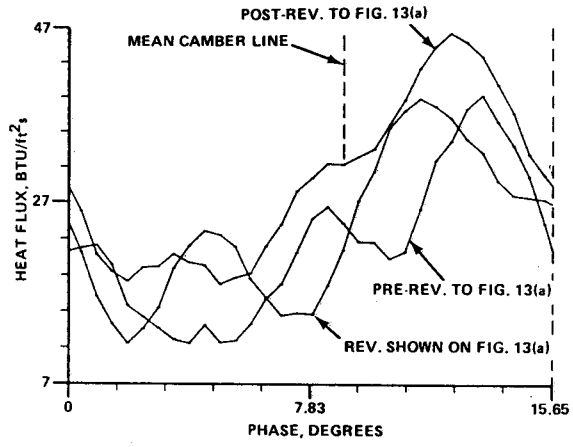

Fig. 13(c) Phase-resolved heat-flux data at 14.9 percent wetted distance on blade suction surface for passage #18 and three successive revolutions

is present on many of the passages but not all of them, as illustrated in Fig. 10, indicating a substantial random component to the flow disturbances at this location.

Contour plots have been constructed from the blade phase-resolved heat-flux distributions. Figure 11(*a*) presents the blade suction contour plot for the geometric stagnation point, 2.07, 10, 16.1, 51, and 78 percent wetted distance for a given blade passage at a selected time. The blade location relative to the vane trailing edge is again referenced according to Fig. 5. The plot illustrates the magnitude of the phase-varying portion of the heat flux, and shows clearly the high degree of correlation of the disturbances. Also illustrated is the very rapid decrease in heat flux as one moves from the geometric stagnation point to the location at 2.07 percent wetted distance. This rapid decrease can be associated with a broadening of the disturbance, a fact also consistent with the reduction in the first harmonic in the blade crossing rate. Figure 11(*b*) presents a similar contour plot for the blade pressure surface constructed from measurements performed at the geometric stagnation point, 12.7, 22, 34.7, and 76 percent wetted distance. Once again, the heat flux falls off rapidly between the stagnation point and 12.7 percent wetted distance. Figures 11(*a*) and 11(*b*) were constructed from heat-flux data taken from the same rotor revolution on the same test run. Note that the characteristics of the unsteady components for the pressure-surface data are different from the corresponding characteristics on the suction-surface results.

5.2 Phase-Resolved Heat-Flux Data on the Blade With Discrete-Hole Vane Injection. A description of the influence of discrete hole injection on the blade steady-state Stanton-number distribution and the influence of vane/blade spacing on this distribution was reported by Dunn and Chupp (1987). While obtaining those steady-state data, a limited quantity of phase-resolved data was also obtained. Figure 12(*a*) presents phase-resolved heat-flux data obtained at 10 percent wetted distance on the blade suction surface at close (0.19 C_s) vane/blade spacing with upstream injection. The injection holes were located at 18.4 percent wetted distance on the vane suction surface and at 71.8 percent wetted distance on the pressure surface. Air at a temperature of 530 R was injected at a flow rate of 0.23 lb/s through the suction surface holes and at 0.20 lb/s through the pressure surface holes for a total of 0.43 lb/s. Comparison of Figs. 12(*a*) and 8(*a*) suggests that the character of the blade flow in the early portion of the passage (see Fig. 5) has been influenced by the cold gas injection. However, the peak heat-flux value again occurred at that phase angle associated with this wake flow and the standard deviations of the time averaged heat flux with and without in-

jection overlapped. Thus, although the presence of injection resulted in a change in the character of the passage heat-flux history, it did not significantly alter the time-averaged level. Figure 12(*b*) is the modulus squared of the heat-flux data reported in Fig. 12(*a*) and this plot clearly shows the fundamental 23 cycles/rev and the first harmonic at 46 cycles/rev. Figure 12(*c*) has been included to demonstrate the nature of the data if seven passages are overlaid. The particular passages are identified by the numbers in circles. The general characteristic of this plot is consistent with the data obtained at other locations and illustrates that an average phase-resolved heat-flux distribution can be obtained from the data. Figure 12(*d*) is another example of the passage phase-resolved heat flux for two successive revolutions of the rotor. These particular data were obtained for passage #13 and illustrate reasonable revolution-to-revolution agreement.

A sample of the blade data obtained with cold gas injection for a vane/blade spacing of 0.5 C_s at 14.9 percent wetted distance on the suction surface is shown in Fig. 13(*a*). The details of the time-averaged data for this configuration are given by Dunn and Chupp (1988). Air was the cooling gas, injected at the locations described in the preceding paragraph, and with a flow rate of 0.13 lb/s through the suction surface holes and 0.11 lb/s through the pressure surface holes. The total weight flow of gas injected through the vane for this case was 0.24 lb/s compared to 0.43 lb/s for the data shown in Fig. 12(*a*). The results shown in Fig. 13(*a*) suggest that the influence of vane/blade spacing was to diffuse the sharp increase in heat flux previously observed to begin in the vicinity of 5 or 6 deg (see Figs. 8(*a*), 9(*a*), and 12(*a*)). At the wider vane/blade spacing, the heat-flux profile increases from 0 deg more slowly, reaching a peak in the vicinity of 12 deg. These results suggest that the blade intersects the vane wake flow at a larger phase angle as would be expected from the geometry of the configuration. The thin-film gage results reported by Dring et al. (1982) illustrate a similar finding for a gap of 0.65 C_s. The modulus squared of the blade data are presented in Fig. 13(*b*) and these results illustrate the fundamental peak at 23 passages/rev. However, because of the diffusing effect of the vane/blade spacing and the greater distance from the stagnation region, the first harmonic is suppressed. The result shown in Fig. 9(*b*) for 16.1 percent wetted distance and close spacing also illustrated a suppressed first harmonic.

Figure 13(*c*) presents the phase-resolved heat-flux history for three successive rotor revolutions for a location of 14.9 percent wetted distance on the blade suction surface. The particular passage selected for this presentation was #18. The phase-resolved data are in reasonably good agreement with each other demonstrating the same type of variation in heat-flux and phase angle as demonstrated for the passage-to-passage variation for a particular revolution.

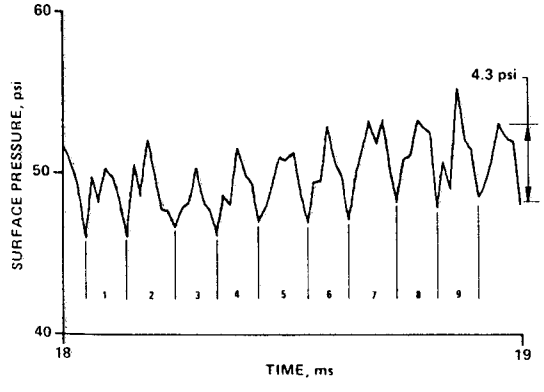

Fig. 14 Blade pressure surface pressure history at 39.3 percent wetted distance

5.3 Time-Resolved Surface Pressure Data on the Blade Pressure Surface. The blade pressure and suction surfaces were instrumented with flush-mounted miniature Kulite pressure transducers. A limited amount of surface pressure data was obtained and a sample of the time-resolved surface pressure history is shown in Fig. 14. The pressure data shown on this figure are for a portion of one revolution (nine passages) obtained from the pressure transducer located at 39.3 percent wetted distance on the blade pressure surface. The pressure data were sampled at a frequency of approximately 70 kHz in constant time intervals. (The one pulse per revolution shaft encoder used to determine the location of the blade relative to the vane trailing edge was not carried on the data system from which the pressure data were obtained.) The steady-state pressure level at this location on the blade surface was approximately 46 psi and the peak-to-peak fluctuation on the time-resolved signal shown on Fig. 14 is on the order of 10 to 15 percent of the time-averaged value. Also it should be noted that the nine passages shown, as defined by the minimum in the pressure data, are not identical in width. This observation is not surprising since the sampling frequency is such that the minimum might have been missed and because the vane is engine hardware and some manufacturing tolerance is to be anticipated. It is planned to obtain significantly more time-resolved and phase-resolved blade pressure data in the near future. These data will be reported as they become available. However, on the basis of the pressure data reported by Dring et al. (1982), and the phase-resolved heat-flux data obtained for this particular blade location in these experiments, the pressure valley is felt to be associated with the vane wake region and the pressure peaks with the passage flow. The magnitude of the fluctuating pressure measured here is of the same order as that reported by Dring et al. (1982).

A heat-flux gage located at 34.7 percent wetted distance on the pressure surface was sufficiently close to the pressure gage location of 39.3 percent to make a meaningful comparison between the general flow characteristics obtained with the two diagnostics. Figure 15 presents the phase resolved heat-flux

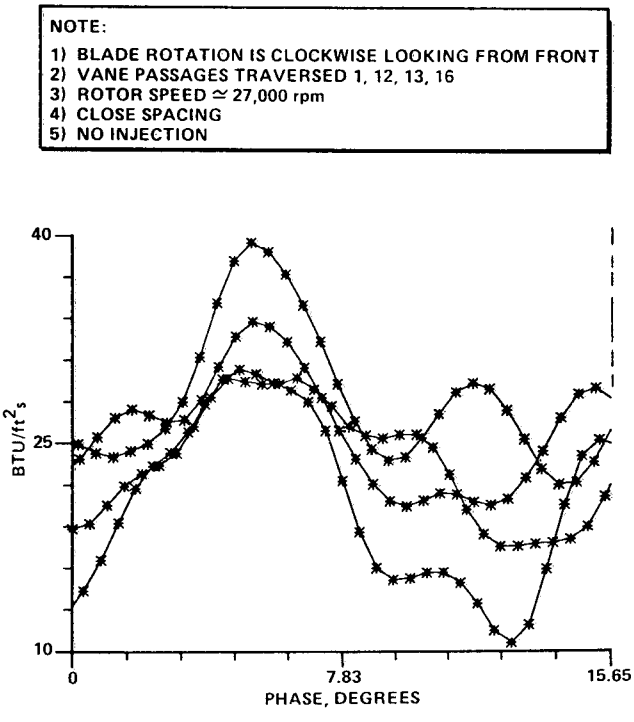

Fig. 15 Phase-resolved heat-flux data at 34.7 percent wetted distance on blade pressure surface

result at 34.7 percent wetted distance. These results were obtained for the same test conditions as the pressure data. The relative location of the vane is again illustrated on Fig. 5. Only a qualitative comparison can be made between Figs. 14 and 15 because the pressure data were not phase resolved as noted above. Comparison of Fig. 15 with Fig. 10 illustrates that farther back on the pressure surface, the general character of this phase-resolved heat-flux history is relatively uniform with peaks occurring at about 6.5 and 12 deg. The minimum again occurs near 0 deg phase angle. However, the general character of the phase-resolved heat-flux history at the farther downstream location appears to be more steady than it was at 12.7 percent wetted distance.

5.4 Consideration of Unsteady Heat-Flux Impact on Blade Durability. The primary purposes of obtaining the unsteady heat-flux and pressure data are to get a better understanding of the flow field around a rotating turbine blade and to obtain validation data for unsteady aerodynamic codes. A separate issue is the impact of the rapidly varying heat flux at the blade surface on blade durability in an engine application. For an uncooled blade such as considered in this experiment, the varying heat flux will be small because the temperature difference between the gas stream and the blade surface is small and durability should not be affected. For a cooled airfoil, the temperature difference can be significant so that the heat flux does vary considerably. Typical heat-flux variation data from this test were corrected to an engine condition with a 1200°F temperature difference between the gas stream and the blade surface. The blade material temperature variation was calculated using an exact solution for a semi-finite solid given by Carslaw and Jaeger (1959). The results show that the surface temperature of a metallic blade would change about 1.5°F in the 21 μs over which the heat flux varied from minimum to maximum (see Fig. 12(*c*) for example). This temperature change dampens quickly into the wall away from the surface (within 0.001 in.). If the blade were coated with a thermal barrier coating, the surface temperature change would be of the order of 6°F and would dampen within 0.00015 in. from the surface. Even though these temperature changes are small, the gradient at the surface is large (3,000 to 40,000°F/in.). Gradients of this magnitude, occurring at such high frequencies, may play a role in determining the fatigue life of blading, particularly since the number of repetitions over the life of an engine is large (typically, 23 vanes × 27,000 rpm × 60 s/min × 1000 h lifetime = 1.3×10^{10}). Further studies, including laboratory testing of blade samples, are required in order to bring these heat transfer results to bear on engine durability problems.

6 Conclusions

Time-resolved or phase-resolved heat-flux data have been presented for the blade of the Teledyne 702 HP turbine. Detailed results have been presented at several locations on the blade. Other results have been shown to illustrate the influence of vane cold-gas injection and vane/blade spacing on the time-resolved blade heat-flux history. All of the blade suction surface data presented illustrate that the peak heat-flux value occurs in that portion of the flow which can be associated with the vane wake. The suction surface boundary layer appears to fluctuate between laminar and turbulent as the blade moves from the passage flow into the vane wake and then out again. The blade pressure surface heat-flux history is shown to be somewhat more unsteady than the suction surface history. The effect of injection at close spacing is shown to influence the early portion of the wake flow resulting in an extended period of low heat flux. The effect of increasing the vane/blade spacing is shown to diffuse the character of the passage heat-flux history.

Acknowledgments

The authors would like to thank Mr. Tom Hajek and Ms. Celina Kosier, both formerly of Teledyne CAE, for many helpful discussions during the initial efforts of this research program. The authors would also like to thank Prof. William J. Rae of the State University of New York at Buffalo for many helpful discussions during the course of this work. The research described in this paper was supported by Teledyne CAE Independent Research and Development funds. The phase-resolved data analysis procedure was developed under support from NASA Lewis Research Center, Grant No. NAG3-581 and monitored by Mr. Kas Civinskas.

References

Adamczyk, J. J., 1985, "Model Equation for Simulating Flows in Multistage Turbomachinery," ASME Paper No. 85-GT-226.

Anand, A. K., and Lakshminarayana, R., 1978, "An Experimental Study of Three-Dimensional Turbulent Boundary Layer and Turbulence Characteristics Inside a Turbomachinery Passage," ASME *Journal of Engineering for Power*, Vol. 100, pp. 676-690.

Binder, A., Forster, W., Kruse, H., and Rogge, H., 1985, "An Experimental Investigation Into the Effect of Wakes on the Unsteady Turbine Rotor Flow," ASME *Journal of Engineering for Gas Turbines and Power*, Vol. 107, pp. 458-466.

Binder, A., Forster, W., Mach, K., and Rogge, H., 1987, "Unsteady Flow Interaction Caused by Stator Secondary Vortices in a Turbine Rotor," ASME JOURNAL OF TURBOMACHINERY, Vol. 109, pp. 251-257.

Carslaw, H. S., and Jaeger, J. C., 1959, *Conduction of Heat in Solids*, 2nd ed., Oxford University Press, New York, p. 72.

Doorly, D. J., and Oldfield, M. L. G., 1985, "Simulation of the Effects of Shock Wave Passing on a Turbine Rotor Blade," ASME *Journal of Engineering for Gas Turbines and Power*, Vol. 107, pp. 998-1006.

Dring, R. P., Blair, M. F., and Josyln, H. D., 1980, "An Experimental Investigation of Film Cooling on a Turbine Rotor Blade," *Journal of Engineering for Power*, Vol. 102, pp. 81-87.

Dring, R. P., and Joslyn, H. D., 1981, "Measurement of Turbine Rotor Blade Flows," ASME *Journal of Engineering for Power*, Vol. 103, pp. 400-405.

Dring, R. P., Joslyn, H. D., Hardin, L. W., and Wagner, J. H., 1982, "Turbine Rotor-Stator Interaction," ASME *Journal of Engineering for Power*, Vol. 104, pp. 729-742.

Dunn, M. G., 1986, "Experimental Measurements of Heat-Flux Distribution in a Turbine Stage With Upstream Disturbances," NASA CP-2436, Vol. I, pp. 614-636.

Dunn, M. G., and Chupp, R. E., 1987, "Influence of Vane/Blade Spacing and Cold-Gas Injection on Vane and Blade Heat-Flux Distributions for the Teledyne 702 HP Turbine Stage," Paper No. AIAA 87-1915, 23rd Joint Propulsion Conf., San Diego, CA.

Dunn, M. G., and Chupp, R. E., 1988, "Time-Averaged Heat-Flux Distributions and Comparison With Prediction for the Teledyne 702 HP Turbine Stage," ASME JOURNAL OF TURBOMACHINERY, Vol. 110, pp. 51-56.

Dunn, M. G., and Hause, A., 1982, "Measurements of Heat Flux and Pressure in a Turbine Stage," *Journal of Engineering for Power*, Vol. 104, pp. 76-82.

Dunn, M. G., Lukis, G., Urso, M., Hiemenz, R. J., Orszulak, R. L., and Kay, N. J., 1984a, "Instrumentation for Gas Turbine Research in Short-Duration Facilities," Paper No. 841504, Aerospace Congress and Exposition (SAE), Long Beach, CA.

Dunn, M. G., Rae, W. J., and Holt, J. L., 1984b, "Measurement and Analysis of Heat Flux Data in a Turbine Stage: Part II—Discussion of Results and Comparison With Predictions," *Journal of Engineering for Gas Turbines and Power*, Vol. 106, pp. 234-240.

Dunn, M. G., George, W. K., Rae, W. J., Woodward, S. H., Moeller, J. C., and Seymour, P. J., 1986, "Heat Flux Measurements for the Rotor of a Full-Stage Turbine: Part II—Technique and Typical Time-Resolved Measurements," ASME JOURNAL OF TURBOMACHINERY, Vol. 108, pp. 98-107.

Evans, R. L., 1978, "Boundary Layer Development on an Axial-Flow Compressor Stator Blade," ASME *Journal of Engineering for Power*, Vol. 100, pp. 287-293.

George, W. K., Rae, W. J., Seymour, P. J., and Sonnenmeier, J. K., 1987, "An Evaluation of Analog and Numerical Techniques for Unsteady Heat Transfer Measurements With Thin-Film Gauges in Transient Facilities," *Proc. of the 1987 ASME-JSME Thermal Engineering Joint Conf.*, pp. 611-617.

Giesing, J. P., 1968, "Nonlinear Interaction of Two Lifting Bodies in Arbitrary Unsteady Motion," ASME *Journal of Basic Engineering*, Vol. 90, pp. 387-394.

Gorton, C. A., and Lakshminarayana, B., 1976, "A Method of Measuring the Three-Dimensional Mean Flow and Turbulence Quantities Inside a Rotating Turbomachinery Passage," ASME *Journal of Engineering for Power*, Vol. 98, pp. 137–146.

Hodson, H. P., 1984, "Boundary Layer and Loss Measurements on the Rotor of an Axial-Flow Turbine," ASME *Journal of Engineering for Gas Turbines and Power*, Vol. 106, pp. 391–399.

Hodson, H. P., 1985a, "Boundary-Layer Transition and Separation Near the Leading Edge of a High-Speed Turbine Blade," ASME *Journal of Engineering for Gas Turbines and Power*, Vol. 107, pp. 127–134.

Hodson, H. P., 1985b, "Measurements of Wake-Generated Unsteadiness in the Rotor Passages of Axial Flow Turbine," ASME *Journal of Engineering for Gas Turbines and Power*, Vol. 107, pp. 467–476.

Joslyn, H. D., Caspar, J. R., and Dring, R. P., 1985, "Inviscid Modeling of Turbomachinery Wake Transport," Paper No. AIAA-85-1132.

Kemp, N. H., and Sears, W. R., 1953, "Aerodynamic Interference Between Moving Blade Rows," *J. Aero. Sci.*, Vol. 20, No. 9, pp. 585–597.

Kemp, N. H., and Sears, W. R., 1955, "The Unsteady Forces Due to Viscous Wakes in Turbomachine," *J. Aero. Sci.*, Vol. 22, No. 7, pp. 478–483.

Kerrebrock, J. L., and Mikolajczak, A. A., 1970, "Intra-Stator Transport of Rotor Wakes and Its Effect on Compressor Performance," ASME *Journal of Engineering for Power*, Vol. 92, pp. 359–368.

Lakshminarayana, B., Govindan, T. R., and Reynolds, B., 1982, "Effects of Rotation and Blade Incidence on Properties of Turbomachinery Rotor Wake," *AIAA Journal*, Vol. 20, No. 2, pp. 245–253.

Parker, R., 1969, "Relation Between Blade Row Spacings and Potential Flow Interaction Effects in Turbomechanics," *Proceedings of the Institute of Mechanical Engineering*, Vol. 184, Pt. 3G, No. 11, pp. 1–8.

Sharma, O. P., Butler, T. L., Joslyn, H. D., and Dring, R. P., 1985, "Three-Dimensional Unsteady Flow in an Axial Flow Turbine," *J. of Propulsion*, Vol. 1, No. 1, pp. 28–38.

Taulbee, D. B., Tran, L., and Dunn, M. G., 1989, "Stagnation Point and Surface Heat Transfer for a Turbine Stage: Prediction and Comparison With Data," ASME JOURNAL OF TURBOMACHINERY, this issue.